Multiplexing of OFDM-Based Radar Networks

David Werbunat, Fabio Sgroi, Christina Knill, Benedikt Schweizer, Benedikt Meinecke, Rossen Michev, Jürgen Hasch, Christian Waldschmidt

DOI: 10.1109/RadarConf2147009.2021.9455150

Multiplexing of OFDM-Based Radar Networks

David Werbunat*, Fabio Sgroi*, Christina Knill*, Benedikt Schweizer*, Benedikt Meinecke*,
Rossen Michev†, Jürgen Hasch†, and Christian Waldschmidt*
*Institute of Microwave Engineering, Ulm University, 89081 Ulm, Germany
†Corporate Sector Research and Advance Engineering, Robert Bosch GmbH, 70465 Stuttgart, Germany.
Email: david.werbunat@uni-ulm.de

***Abstract*—Radar networks offer the opportunity of enhancing the radar sensing performance beyond the inherent limitations of single multiple-input multiple-output (MIMO) radars. Different locations of the individual sensor nodes allow for diverse observation angles on the targets. Moreover, in case of a coherent network, such as radar-repeater networks, the direction of arrival (DoA) capabilities are increased. However, a crucial point in exploiting the full potential of a sensor network is the separability of the signals originating from the different sensor nodes during operation, while preserving reasonable radar sensing performance of the individual sensors and the network. In this paper multiplexing methods for an orthogonal frequency-division multiplexing (OFDM)-based radar network are proposed and investigated. The first method combines traditional time and frequency multiplexing, while the second method applies a random assignment in combination with a compressed sensing-based signal evaluation. Both methods are compared with the traditional FDM multiplexing for MIMO-OFDM. For this purpose, performance criteria are proposed and the concepts are evaluated based on measurements and simulations.**

***Index Terms*—Radar network, repeater, multiplexing, frequency division multiplexing (FDM), time division multiplexing (TDM), compressed sensing, orthogonal frequency division multiplexing (OFDM), OFDM radar, OFDM-MIMO radar.**

I. Introduction

Compared to a single co-located multiple-input multiple-output (MIMO) radar sensor, coherent radar networks combine several cooperative sensor nodes. By mounting the nodes side by side this opens up new possibilities. For example, measurements from different aspect angles of objects can be combined to provide an enhanced estimation of the targets properties. Moreover, by exploiting the enhanced aperture of the coherent network, a more precise direction of arrival (DoA) estimation is possible [1], [2].

A promising realization of a coherent sensor network is the radar-repeater network as presented in [1], [3], [4]. It combines one MIMO radar with several repeater nodes. The repeater nodes act as transponders that retransmit the received signal with a frequency shift in the kilohertz range such that coherency is preserved. Fig. 1 illustrates the system concept for one MIMO radar and one repeater node. The monostatic radar response of the MIMO radar sensor is extended with a bistatic signal response from the repeater node, which is eventually evaluated at the MIMO radar after being reflected at the target. This way, a coherent sensor network is established by expanding the radar only by means of simple repeater elements, with no need for a data link or a synchronization

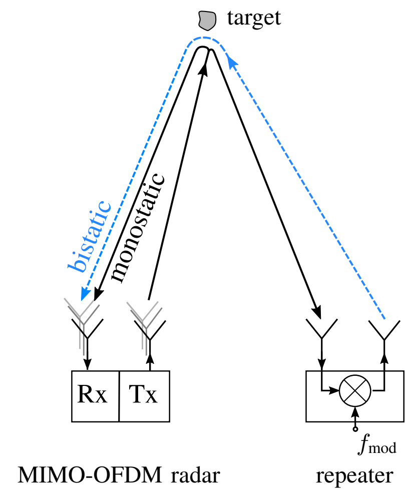

Fig. 1: Concept and signal path of the radar-repeater network, exemplarily shown for one repeater and one target. Figure based on [1].

signal. With its simplicity, this network is an ideal candidate for automotive applications.

Since the MIMO radar receives the superposition of all monostatic and bistatic signals, the benefits of a radar-repeater network can only be fully exploited when those signals are separable at the receveiver node. Through the frequency multiplexing capabilities of the repeater nodes, the application of orthogonal frequency-division multiplexing (OFDM) signals in the network is a proper choice due to its inherent subcarrier-based frequency-division multiplexing (FDM) signal structure. If the repeater nodes shift the signal by an integer multiple of the OFDM subcarrier spacing, the bistatic signal may be interleaved in the OFDM signal structure [1]. However, subcarrier interleaving reduces the unambiguous range and this problem multiplies with additional transmit (Tx) channels and repeaters. Thus, an optimized multiplexing strategy is crucial.

This work contributes to investigations on the new radar-repeater networks by proposing and evaluating adequate multiplexing methods. The high flexibility of OFDM radars is exploited by combining FDM and time-division multiplexing (TDM) approaches while taking into account the special constraints imposed by the repeater elements. Furthermore, a multiplexing method with randomly assigned subcarriers is proposed, which perfectly suits a compressed sensing (CS)-

based range-Doppler (Rv) evaluation. Using suitable key criteria like unambiguous range and velocity, dynamic range, target separability, and network scalability, the different methods are assessed by means of measurements and simulations.

The paper is structured as follows: In section II, the concept of an OFDM-based radar repeater network is introduced. In section III the multiplexing methods are described, followed by their systematical evaluation and comparison in section IV and a conclusion in section V.

II. OFDM-Based Radar-Repeater Network

The radar-repeater network consists of a single radar and several repeater elements. As shown in Fig. 1, there are two types of signals occurring. The monostatic ones are signals with a path from the radar transmitter to the target, where the signal is reflected, and back to the radar receiver. Additionally, bistatic signals are provided by the repeaters. These signals are transmitted by the radar, reflected by a target and received by a repeater. The repeater shifts the frequency and retransmits the signal. Then, the signal is reflected by the targets again and received at the radar receiver. In the following section, this concept is explained in detail, starting with the signal model of the OFDM signal.

A. Signal Model

An OFDM signal is a multicarrier signal consisting of N orthogonal subcarriers with spacing Δf [5]–[7]. In order to ensure the orthogonality of the subcarriers, the OFDM signal consists of M OFDM symbols, each with a length of $T = 1/\Delta f$. Each subcarrier in each OFDM symbol is modulated with a different modulation symbol $d_{\mathrm{Tx}}(n,m) \in \mathbb{C},\ m=0,1,...,M-1,\ n=0,1,...,N-1$. These modulation symbols can be notated as matrix $\mathbf{D}_{\mathrm{Tx}} \in \mathbb{C}^{N\times M}$ with every row representing a subcarrier and every column representing an OFDM symbol. This transmit matrix can be chosen differently for every Tx channel k. In the following, these matrices are denoted as $\mathbf{D}^k_{\mathrm{Tx}},\ k \in 0,1,...,N_{\mathrm{Tx}}-1$, where N_{Tx} is the number of Tx channels. When generating the Tx matrices, the bistatic signals of the repeaters have to be considered. This is done by including zeros in $\mathbf{D}^k_{\mathrm{Tx}}$ and will be explained in detail in Section III.

For every Tx channel, the OFDM signal can be generated by an inverse fast Fourier transform (IFFT). Then, in front of every OFDM symbol, typically a cyclic prefix of length T_{CP} is inserted, increasing the time per OFDM symbol to $T_{\mathrm{OFDM}} = T + T_{\mathrm{CP}}$ [8], [9].

B. Signal Modulation by the Repeater

The repeaters consist of a double-sideband (DSB) mixer and amplifiers [10], [11]. Based on their receive (Rx) signal $x_{\mathrm{Rp}}(t)$, their modulated Tx signal can be described as [1]

$$y_{\mathrm{Rp}}(t) = x_{\mathrm{Rp}}(t)\,\alpha_{\mathrm{Rp}} \left(\mathrm{e}^{+\mathrm{j}(f_{\mathrm{mod}}t+\phi_{\mathrm{mod}})} + \mathrm{e}^{-\mathrm{j}(f_{\mathrm{mod}}t+\phi_{\mathrm{mod}})}\right). \quad (1)$$

The factor $\alpha_{\mathrm{Rp}} \in \mathbb{C}$ represents the phase shift and signal gain due to the repeater hardware, f_{mod} the modulation frequency, and ϕ_{mod} the phase shift due to the modulation signal. To provide an integer subcarrier shift, f_{mod} is chosen as [1]

$$f_{\mathrm{mod}} = h\,\Delta f, \qquad h \in \mathbb{Z} \setminus 0. \quad (2)$$

The factor h equals the shift in multiples of the subcarrier spacing. Using double-sideband (DSB) mixers, the signal is shifted not only by $h_{\mathrm{I}} = h$ subcarriers leading to the upper sideband (USB), but also by $h_{\mathrm{II}} = -h$ subcarriers for the lower sideband (LSB). Every multiplexing method is limited by these capabilities of the repeaters to modify the signal.

C. Radar Processing

Principally, the OFDM signal is evaluated similar to standard OFDM radar processing [8], [9]. However, some adaptions are made especially for the bistatic signals, as shown in the signal processing chart in [1, Fig. 3].

For both the monostatic and the bistatic evaluation at every receiver the Rx signal is transformed to symbol domain at first. This way, a combined symbol matrix $\mathbf{D}_{\mathrm{Rx}}$ containing the information from the signals of all Tx channels and every network node is gained. For further processing, the transmitted modulation symbols have to be removed and $\mathbf{D}_{\mathrm{Rx}}$ has to be separated into one matrix for each mono- and bistatic signal. Thus the monostatic division matrix for the kth Tx channel is calculated by

$$\mathbf{D}^k_{\mathrm{Div}} = \mathbf{D}_{\mathrm{Rx}} \odot \left(\mathbf{D}^k_{\mathrm{Tx}}\right)^*, \quad (3)$$

where the operator $\odot$ represents an elementwise multiplication and $(\cdot)^*$ the complex conjugate. Due to the zeros included in $\mathbf{D}^k_{\mathrm{Tx}}$ for modulation symbols not assigned to the kth Tx channel, with orthogonal subcarriers there is no influence of the signals from other Tx channels and the repeater nodes. The bistatic signals received at the radar are based on the same Tx matrix $\mathbf{D}^k_{\mathrm{Tx}}$ but have been shifted by h subcarriers. This equals a shift of the modulation symbol matrix in subcarrier direction, leading to the shifted Tx matrix $\mathbf{D}^{k,h}_{\mathrm{Tx}}$ and a division matrix $\mathbf{D}^{k,h}_{\mathrm{Div}}$. Factor h can be either h_{I} or h_{II} of any repeater. Therefore, for every Tx channel and every sideband of every repeater, an independent division matrix can be generated, leading to an independent Rv-evaluation each.

The velocity evaluation can be performed by a rowwise fast Fourier transform (FFT) on $\mathbf{D}_{\mathrm{Div}}$, while the range evaluation is performed by a columnwise IFFT [8], [9]. For the bistatic processing, furthermore, the influence of the subcarrier shift has to be corrected [1].

III. Multiplexing Methods

Through multiplexing, the orthogonality in time and frequency has to be provided. This is equivalent to every element in $\mathbf{D}_{\mathrm{Rx}}$ being only affected by either one radar Tx channel or one repeater. In the following section, different multiplexing methods ensuring this by a proper assignment of the modulation symbols in $\mathbf{D}^k_{\mathrm{Tx}}$ are presented.

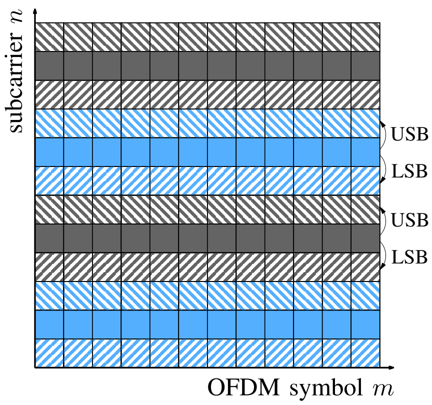

(a) FDM.

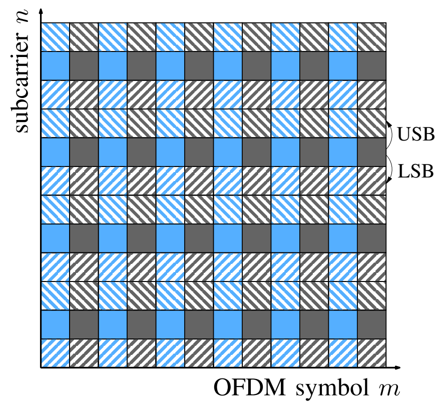

(b) TFDM.

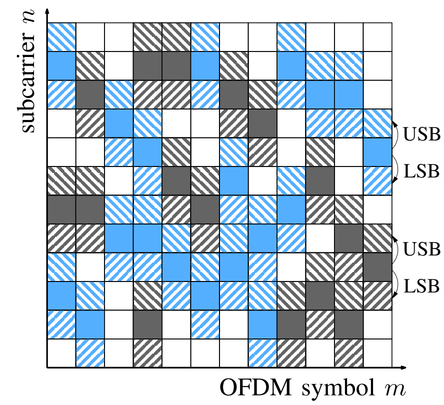

(c) RFDM.

Fig. 2: Modulation symbol assignment of the proposed multiplexing methods, examplary for a network with two Tx channels and one DSB repeater (Tx1: ■, Tx2: ■, unassigned: □).

A. Frequency-Division Multiplexing

The straight-forward multiplexing method in an OFDM network is the assignment of different subcarriers to different network nodes and Tx channels, as it is proposed in [1], [9], [12]. In a radar-repeater network, this is done by assigning a set of subcarriers to the radar and providing free subcarriers for the repeater node, which is shown exemplarily in Fig. 2a for one repeater and two Tx channels. Every repeater shifts the signal by $\pm(n_{\mathrm{RP}}+1)$ subcarriers, where $n_{\mathrm{RP}}=0,1,\ldots,N_{\mathrm{Rp}}-1$ is the number of the repeater. The subcarriers assigned to the radar then are mapped regularly to the different Tx channels. Thus, huge spacings between the subcarriers assigned to the same Tx channel occur.

B. Combined Time- and Frequency-Division Multiplexing

In order to reduce the spacing between two subcarriers used by the same Tx channel and network node, a combined time- and frequency-division multiplexing (TFDM) is proposed. For TFDM, the transmit channels are multiplexed in time instead of frequency, while the repeaters perform FDM. The resulting pattern is shown exemplarily in Fig. 2b. The spacing in subcarrier direction only depends on the number of repeaters and is significantly reduced. However, this is at the expense of the spacing in direction of the OFDM symbols.

C. Random Multiplexing with Compressed Sensing-Based Rv-Evaluation

As alternative to the regular assignment strategies FDM and TFDM, a CS facilitating random assignment of the modulation symbols to the channels is proposed. In the following, this multiplexing method is called random frequency-division multiplexing (RFDM).

However, the limitations of the repeaters regarding their signal modulation have to be considered, as the USB and LSB of the repeaters are still regularly shifted to a subcarrier above and below of one modulation symbol used by the radar. Thus, in addition to the non-regular allocated modulation symbols of the radar Tx channels and the symbols assigned to the repeater nodes, unassigned modulation symbols remain.

Similar to CS-based random multiplexing for a single MIMO radar [13], this multiplexing strategy suits for an Rv-evaluation with CS. Considering the finite number of targets, with the Rv-domain a sparse domain exists and the missing samples in $\mathbf{D}_{\mathrm{Div}}$ can be reconstructed [14], [15]. In this work, this optimization problem is solved by a 2D-version of complex approximate message passing (CAMP) [16] while using the 2D-FFT as transformation in the sparse domain. Thus as proposed in [17] the reconstruction in range and velocity direction is combined.

IV. Comparison & Evaluation

In order to compare the multiplexing methods systematically, several evaluation criteria are introduced. The unambiguous region is critical for the unambiguous detection of targets and is strongly influenced by the multiplexing method. The dynamic performance determines whether weak targets are detectable or not. Furthermore, the network scalability determines how the radar performance is affected when increasing the number of Tx channels or repeaters.

The evaluation is performed using simulations and measurements. For the measurements, a MIMO-OFDM frontend with $N_{\mathrm{Tx}}=4$ transmit channels is used in combination with a Xilinx RFSoC to generate and store the baseband signals [18], [19]. The radar operates at the automotive frequency band at 77 GHz. The OFDM parameters for the measurements are listed in Table I. The radar is combined with $N_{\mathrm{Rp}}=2$ repeater nodes, each composed of amplifiers and a mixer and similar to the repeaters from [10]. The measurement setup is shown in Fig. 3.

A. Unambiguous Region

Maximizing the unambiguous regions is crucial to preserve the ability to estimate the correct velocity and range of the

TABLE I: Radar parameters.

Parameter		Measurements	Simulations
Number of Tx channels	N_{Tx}	4	2
Number repeaters	N_{Rp}	2	2
Carrier frequency	f_{c}	77 GHz	–
Subcarrier spacing	Δf	400 kHz	500 kHz
Bandwidth	B	409.6 MHz	750 MHz
Number of subcarriers	N	1024	1500
Number of OFDM symbols	M	2048	1000
Range resolution	ΔR	0.37 m	0.2 m
Velocity resolution	Δv_{rel}	0.33 $\frac{\mathrm{m}}{\mathrm{s}}$	0.81 $\frac{\mathrm{m}}{\mathrm{s}}$
Unambiguous range (SISO)	R_{ua}	374.7 m	299.8 m
Unambiguous velocity (SISO)	$v_{\mathrm{rel,ua}}$	±337.5 $\frac{\mathrm{m}}{\mathrm{s}}$	±324 $\frac{\mathrm{m}}{\mathrm{s}}$
Mod. frequency repeater 1	$f_{\mathrm{mod},0}$	400 kHz	500 kHz
Mod. frequency repeater 2	$f_{\mathrm{mod},1}$	800 kHz	1000 kHz

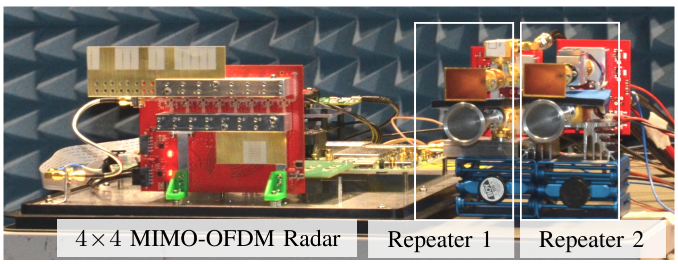

Fig. 3: Measurement setup.

targets. Since range and velocity are evaluated by means of an FFT and thus, the Nyquist criterion applies, the subcarrier spacing Δf and the OFDM symbol repetition interval T_{OFDM} directly correspond to the unambiguous region in range and velocity, respectively [20], [21]. For multiplexing the modulation symbols are allocated to the different Tx channels and repeaters. Thus, the effective subcarrier spacing $\Delta\tilde{f} = \Delta n_{\mathrm{Tx}}\,\Delta f$ and the effective time interval $\tilde{T}_{\mathrm{OFDM}} = \Delta m_{\mathrm{Tx}}\,T_{\mathrm{OFDM}}$ between two modulation symbols assigned to the same signal are increased. This leads to the effective unambiguous range $\tilde{R}_{\mathrm{ua}}$ and velocity $\tilde{v}_{\mathrm{rel,ua}}$ decreased by the reduction factors Δn_{Tx} and Δm_{Tx}, respectively. Both factors differ depending on the multiplexing method.

For FDM the radar's Tx channels as well as the USB and LSB of every repeater are separated in frequency only. Thus, the effective subcarrier spacing is increased by

$$\Delta n_{\mathrm{Tx}}^{\mathrm{FDM}} = N_{\mathrm{Tx}}\,(2N_{\mathrm{Rp}} + 1)\,, \tag{4}$$

while the effective time interval $\tilde{T}_{\mathrm{OFDM}}^{\mathrm{FDM}} = T_{\mathrm{OFDM}}$ is identical to the single-input single-output (SISO) case. In the measurements, the network with $N_{\mathrm{Tx}} = 4$ and $N_{\mathrm{Rp}} = 2$ leads to a reduction by $\Delta n_{\mathrm{Tx}}^{\mathrm{FDM}} = 20$. Thus, $\tilde{R}_{\mathrm{ua}}^{\mathrm{FDM}}$ equals 18.7 m considering the OFDM parameters from Table I. The resulting repetitions in the range profile are shown in Fig. 4a, where measurements of a single target at a distance of 2.4 m are presented.

For TFDM only the repeaters are multiplexed in frequency. Thus, the reduction factor becomes

$$\Delta n_{\mathrm{Tx}}^{\mathrm{TFDM}} = 2N_{\mathrm{Rp}} + 1 \tag{5}$$

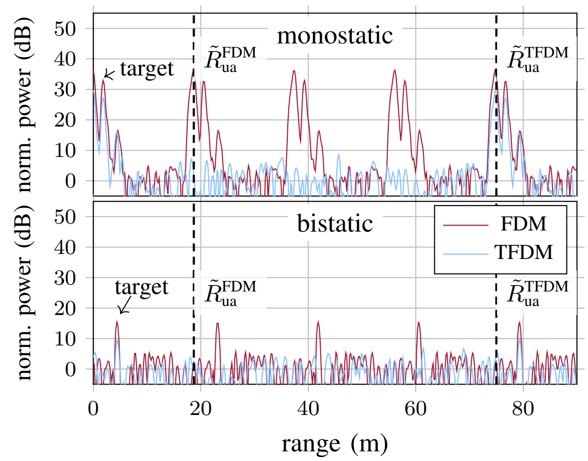

(a) FDM and TFDM.

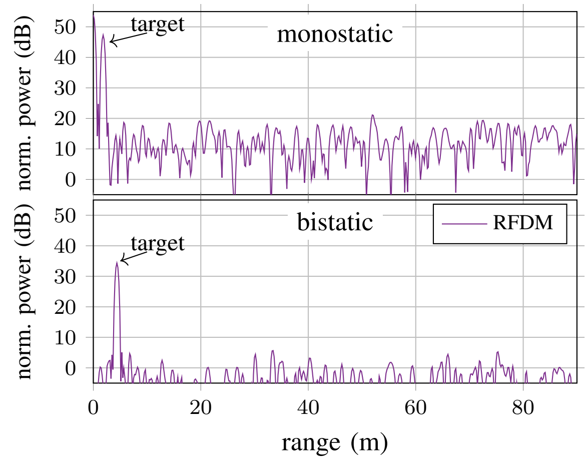

(b) RFDM.

Fig. 4: Measurement results of a scenario with one target at 2.4 m. The mono- and bistatic range profile ($v_{\mathrm{rel}} = 0\,\frac{\mathrm{m}}{\mathrm{s}}$) are plotted for different multiplexing methods. As the bistatic signal is reflected at the targets twice, the range is approximately double the range as in the monostatic case.

and in case of the network with $N_{\mathrm{Rp}} = 2$ used for measurements $\tilde{R}_{\mathrm{ua}}^{\mathrm{TFDM}}$ equals 75 m. However, this has the drawback that also the unambiguous velocity is reduced by

$$\Delta m_{\mathrm{Tx}}^{\mathrm{TFDM}} = N_{\mathrm{Tx}}\,. \tag{6}$$

As OFDM radars typically have a very large unambiguous velocity compared to frequency-modulated continuous wave (FMCW) radars [22], this reduction is usually tolerable. In the measurements shown in Fig. 4a, the unambiguous velocity of TFDM equals $\tilde{v}_{\mathrm{rel,ua}}^{\mathrm{TFDM}} = 84.4\,\frac{\mathrm{m}}{\mathrm{s}}$. By using RFDM the same unambiguous region as with a SISO radar can be achieved, as the missing samples are reconstructed by CS. Thus, the range profile shown in Fig. 4b is free of repetitions.

B. Dynamic Performance

The dynamic performance describes the capability of the sensors to detect weak targets. While the dynamic range is determined by restrictions due to the signal-to-noise ratio (SNR) required to detect a target, the target separability describes the limits in the detection of two close-by targets.

1) Dynamic Range: One factor determining the dynamic range is the integration gain, which directly influences the SNR and is determined by the total number of symbols of the OFDM frame coherently integrated at the receiver per channel. Thus, the integration gain equals

$$G_{\text{int}} = \frac{N\,M}{S} \tag{7}$$

where S is called sparsity factor. For FDM and TFDM, this is given by

$$S^{\text{FDM}} = S^{\text{TFDM}} = N_{\text{Tx}}\,(2N_{\text{Rp}} + 1)\,. \tag{8}$$

For the bistatic signals of the repeaters, the integration gain is the same. For RFDM additional non-assigned modulation symbols are unavoidable in order to provide a random assignment of the modulation symbols. In this work, the sparsity of RFDM is given by $S^{\text{RFDM}} \approx 2S^{\text{FDM}}$. However, as the CS algorithm estimates the sparse elements in the Rv-evaluation, this leads to a higher pseudo-SNR [14], which is visible when comparing the high SNR in Fig. 4b with the lower SNR in Fig. 4a.

The second factor is the average Tx power of each transmitter. Using FDM or RFDM each channel transmits all the time. Regardless the assigned modulation symbols, each channel transmits with the output power P_{out} allowed by the power amplifier. Thus, the average output power per channel for FDM and RFDM equals $P_{\text{avg}}^{\text{TFDM}} = P_{\text{avg}}^{\text{RFDM}} = P_{\text{out}}$. In contrast, for TFDM every transmitter is only active an N_{Tx}th of the time, leading to a reduced $P_{\text{avg}}^{\text{TFDM}} = P_{\text{out}}/N_{\text{Tx}}$. In the measurements, due to the four Tx channels this leads to a power reduction by 6 dB, which can be seen by the difference in the target peak power in Fig. 4a.

2) Target Separability: For RFDM the random spacings in the modulation symbol assignment lead to artifacts in the Rv-spectrum. Although the sparse samples are reconstructed by a CS algorithm, there is no chance for the algorithm to reconstruct a weak target next to a strong one if the weak target is covered by strong artifacts from the other target.

In order to evaluate this effect, simulations of targets at the same range with their velocities being different, but equally off-grid, are performed. While the radar cross section (RCS) of the stronger target is fix, the RCS of the weaker target is varied, leading to an RCS difference ΔRCS. The results are evaluated with a constant false alarm rate (CFAR) algorithm and the detection probability of the weaker target P_{D} is determined. In Fig. 5, the resulting P_{D} vs. ΔRCS is shown for different velocity differences $\Delta v_{\text{rel,target}}$. In the monostatic evaluation for RFDM, independently of $\Delta v_{\text{rel,target}}$ the second target is not detectable for $\Delta\text{RCS} > 30\,\text{dB}$. In contrast, for TFDM besides the minimum SNR no such limit seems to exist. However, it must be noted that this is only an exemplary result, as it depends on both the CS and CFAR algorithm and their parameters. In the bistatic evaluation, the detection

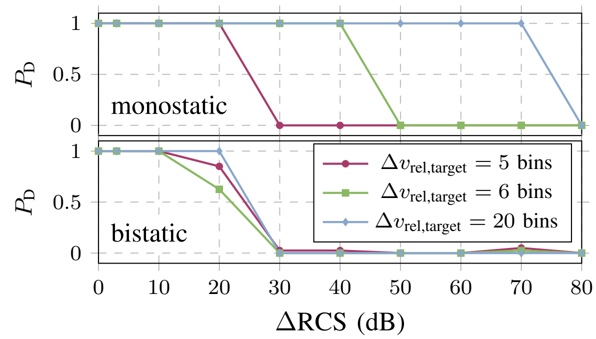

(a) TFDM.

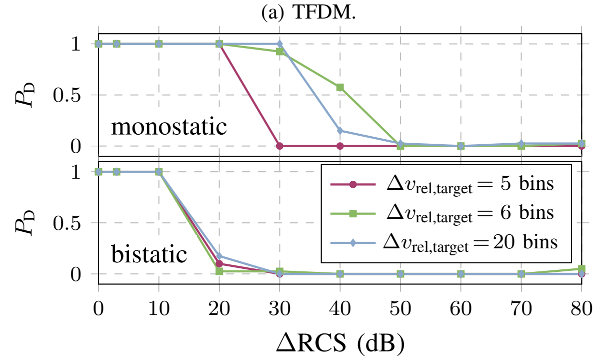

(b) RFDM.

Fig. 5: Simulation results for two targets with a velocity difference of Δv_{rel}. The RCS of the weaker target is plotted vs. its detection probability P_{D}. P_{D} is determined based on 20 simulations per scenario.

is limited by the noise floor, with a stronger limitation for RFDM. Thus, the detection of the weaker target is limited almost independently from $\Delta v_{\text{rel,target}}$.

C. Network Scalability

The network scalability describes how the radar performance is affected when different numbers of transmitter or repeater nodes are used. For FDM $\tilde{R}_{\text{ua}}$ is decreased when increasing the number of Tx channels N_{Tx} as well as when increasing the number of repeaters N_{Rp}, leading to a rapidly reduced unambiguous range. Using TFDM, the unambiguous range is only reduced when increasing N_{Rp}, but the unambiguous velocity is reduced by factor N_{Tx}. These influences are summarized in Table II.

When exemplarily considering a network with $N_{\text{Tx}} = 4$ and $N_{\text{Rp}} = 4$, and the measurement parameters from Table I, for FDM the range ambiguity is reduced by an increased $\Delta n_{\text{Tx}}^{\text{FDM}} = 36$. This leads to a barely practical $\tilde{R}_{\text{ua}}^{\text{FDM}} = 10.4\,\text{m}$. Using TFDM the unambiguous range is only reduced by $\Delta n_{\text{Tx}}^{\text{TFDM}} = 9$ to $\tilde{R}_{\text{ua}}^{\text{TFDM}} = 41.6\,\text{m}$, which could be acceptable for short range applications.

In contrast, when using RFDM, the unambiguous range and velocity are not affected by increasing N_{Tx} or N_{Rp}. However, the sparsity is increased, leading to a higher pseudo-SNR, as more samples are reconstructed. Nevertheless, this is limited to a maximum sparsity, where the CS algorithm is not able

TABLE II: Network scalibility.

	FDM	TFDM	Random
$N_{\text{Tx}} \uparrow$	$\tilde{R}_{\text{ua}}^{\text{FDM}} \downarrow$, $S^{\text{FDM}} \uparrow$	$\tilde{v}_{\text{rel,ua}}^{\text{TFDM}} \downarrow$, $S^{\text{TFDM}} \uparrow$	$S^{\text{RFDM}} \uparrow$
$N_{\text{Rp}} \uparrow$	$\tilde{R}_{\text{ua}}^{\text{FDM}} \downarrow$, $S^{\text{FDM}} \uparrow$	$\tilde{R}_{\text{ua}}^{\text{TFDM}} \downarrow$, $S^{\text{TFDM}} \uparrow$	$S^{\text{RFDM}} \uparrow$

TABLE III: Comparison of the multiplexing methods with respect to the evaluation criteria from Section IV.

	FDM	TFDM	Random
Unambiguous range	– –	–	+
Unambiguous velocity	+	–	+
Dynamic range	+	(–)	(–)
Target separability	+	+	–
Network scalability	– –	–	+

to reconstruct the targets anymore [16]. This limit depends on the chosen algorithm as well as its parametrization.

D. Comparison

Table III summarizes the advantages and disadvantages of the multiplexing methods. The choice of the most suitable multiplexing method, however, depends on the network setup and the measurement scenario.

Considering automotive scenarios, in a highway scenario large unambiguous ranges and velocities must be covered. In this case, RFDM is the proper choice, as in contrast to FDM and TFDM, the unambiguous range and velocity are not reduced compared to a SISO radar with the same parameters.

In urban scenarios it is crucial to detect weak and vulnerable targets. Therefore, RFDM is disadvantageous compared to the other multiplexing methods due to its limited target separability. As TFDM not only offers a good dynamic performance, but also reasonable unambiguous regions, it is very likely the most universal option in this scenario. However, for specific applications with ultra short measurement ranges, FDM could be favorable due to its superior dynamic range.

V. Conclusion

In this work, different methods for multiplexing an OFDM-based radar-repeater network were proposed and evaluated. In the first method, TFDM, the repeaters are multiplexed in frequency, while the Tx channels are multiplexed in time. It achieves a good dynamic performance with reasonable restrictions in the unambiguous range and velocity. The second method, RFDM, leads to a CS-friendly time-frequency sampling pattern for Rv-evaluation. By means of the CS algorithm, it is possible the retain the full unambiguous regions at the expense of degraded target separability.

However, due to the advantages of a digital radar, this is not an either-or, since it is possible to change the multiplexing method on the fly. The radar only has to adapt the baseband signal, which is feasible from one measurement to another. The advantages of TFDM and RFDM can even be combined by merging the information of two consecutive measurements with different multiplexing methods.

References

[1] D. Werbunat, B. Meinecke, B. Schweizer, J. Hasch, and C. Waldschmidt, "OFDM-based radar network providing phase coherent DOA estimation," *IEEE Trans. Microw. Theory Techn.*, 2020.

[2] A. Dürr, R. Kramer, D. Schwarz, M. Geiger, and C. Waldschmidt, "Calibration-based phase coherence of incoherent and quasi-coherent 160-GHz MIMO radars," *IEEE Trans. Microw. Theory Techn.*, pp. 1–1, 2020.

[3] B. Meinecke, M. Steiner, J. Schlichenmaier, J. Hasch, and C. Waldschmidt, "Coherent multistatic MIMO radar networks based on repeater tags," *IEEE Trans. Microw. Theory Techn.*, pp. 1–9, 2019.

[4] D. Werbunat, B. Meinecke, M. Steiner, and C. Waldschmidt, "Phase recovery in sensor networks based on incoherent repeater elements," in *Proc. IEEE MTT-S Int. Microwave Symp.*, 2020, pp. 1149–1152.

[5] R. W. Chang, "Synthesis of band-limited orthogonal signals for multichannel data transmission," *Bell System Technical Journal*, vol. 45, no. 10, pp. 1775–1796, 1966.

[6] N. Levanon, "Multifrequency complementary phase-coded radar signal," *IEEE Proc. – Radar, Sonar and Navigation*, vol. 147, no. 6, p. 276, 2000.

[7] ——, "Multifrequency radar signals," in *Record of the IEEE Int. Radar Conf. [Cat. No. 00CH37037]*, 2000.

[8] C. Sturm and W. Wiesbeck, "Waveform design and signal processing aspects for fusion of wireless communications and radar sensing," *Proc. IEEE*, vol. 99, no. 7, pp. 1236–1259, 2011.

[9] C. Sturm, Y. L. Sit, M. Braun, and T. Zwick, "Spectrally interleaved multi-carrier signals for radar network applications and multi-input multi-output radar," *IET Radar, Sonar & Navigation*, vol. 7, no. 3, pp. 261–269, 2013.

[10] M. Sadegh Dadash, J. Hasch, P. Chevalier, A. Cathelin, N. Cahoon, and S. P. Voinigescu, "Design of low-power active tags for operation with 77–81-GHz FMCW radar," *IEEE Trans. Microw. Theory Techn.*, vol. 65, no. 12, pp. 5377–5388, 2017.

[11] M. Sadegh Dadash, J. Hasch, P. Chevalier, A. Cathelin, and S. P. Voinigescu, "A W-band active millimeter-wave tag IC with wake-up function," in *IEEE MTT-S Int. Microwave Symp.* IEEE, 2017.

[12] Z. Lin and Z. Wang, "Interleaved OFDM signals for MIMO radar," *IEEE Sensors J.*, vol. 15, no. 11, pp. 6294–6305, 2015.

[13] C. Knill, F. Roos, B. Schweizer, D. Schindler, and C. Waldschmidt, "Random multiplexing for an MIMO-OFDM radar with compressed sensing-based reconstruction," *IEEE Microw. and Wireless Compon. Lett.*, vol. 29, no. 4, pp. 300–302, 2019.

[14] C. Knill, B. Schweizer, S. Sparrer, F. Roos, R. F. H. Fischer, and C. Waldschmidt, "High range and Doppler resolution by application of compressed sensing using low baseband bandwidth OFDM radar," *IEEE Trans. Microw. Theory Techn.*, vol. 66, no. 7, pp. 3535–3546, 2018.

[15] M. A. Hadi, S. Alshebeili, K. Jamil, and F. E. Abd El-Samie, "Compressive sensing applied to radar systems: an overview," *Signal, Image and Video Processing*, vol. 9, no. 1, pp. 25–39, 2015.

[16] A. Maleki, L. Anitori, Z. Yang, and R. G. Baraniuk, "Asymptotic analysis of complex lasso via complex approximate message passing (camp)," *IEEE Trans. on Information Theory*, vol. 59, no. 7, pp. 4290–4308, 2013.

[17] F. Roos, P. Hügler, C. Knill, L. L. Tovar Torres, N. Appenrodt, J. Dickmann, and C. Waldschmidt, "Comparison of 2D and 3D compressed sensing for high-resolution TDM-MIMO radars," in *16th European Radar Conf. (EuRAD)*, 2019, pp. 253–256.

[18] B. Farley, J. McGrath, and C. Erdmann, "An all-programmable 16-nm RFSoC for digital-RF communications," *IEEE Micro*, vol. 38, no. 2, pp. 61–71, 2018.

[19] B. Schweizer, A. Grathwohl, G. Rossi, P. Hinz, C. Knill, S. Stephany, H. J. Ng, and C. Waldschmidt, "The fairy tale of simple all-digital radars: How to deal with 100 Gbit/s of a digital millimeter-wave MIMO radar on an FPGA," *IEEE Microwave Magazine*, accepted for publication.

[20] C. Sturm, E. Pancera, T. Zwick, and W. Wiesbeck, "A novel approach to OFDM radar processing," in *IEEE Radar Conf.*, 2009, pp. 1–4.

[21] Y. L. Sit, C. Sturm, and T. Zwick, "Doppler estimation in an OFDM joint radar and communication system," in *German Microwave Conf.* IEEE, 2011, pp. 1–4.

[22] M. Kronauge and H. Rohling, "New chirp sequence radar waveform," *IEEE Trans. Aerosp. Electron. Syst.*, vol. 50, no. 4, pp. 2870–2877, 2014.